PCCP

ROYAL SOCIETY OF CHEMISTRY

PAPER

Cite this: *Phys. Chem. Chem. Phys.*, 2025, **27**, 3854

Exploring ground-state and ionization potentials of the $H_2CO\cdots HNO$ dimers†

Gabriel L. C. de Souza *[ab] and Kirk A. Peterson *[c]

Received 21st November 2024,
Accepted 15th January 2025

DOI: 10.1039/d4cp04442h

rsc.li/pccp

In this work, we performed an investigation on the structures and ionization potentials (IPs) of the $H_2CO\cdots HNO$ dimer. The ground-state properties of six conformations were explored using the coupled-cluster with single, double, and perturbative triple excitations, CCSD(T), approach with large correlation consistent basis sets. Conformation III presented the strongest hydrogen-bonding interaction (with the NH$\cdots$O distance being 2.016 Å) and was assigned as the most stable among the conformations. In addition, twelve lowest-lying IPs of all the $H_2CO\cdots HNO$ conformations were determined using the equation-of-motion ionization potential coupled-cluster with single and double excitations method (EOMIP-CCSD) combined with correlation consistent basis sets, extrapolation to the complete basis set limit, and consideration of core correlation effects. The first IP of conformation III was determined to be 10.46 eV, while the corresponding values for conformations I and II were found as being lower than the value obtained for conformation III by 0.41 eV and 0.24 eV, respectively. These differences (that were also noticed for other low-lying IPs) may be helpful for the assignments of experimental results and, thus, it is expected that the outcomes from this work may serve as motivation for other experimental and theoretical investigations involving $H_2CO\cdots HNO$ dimers (particularly studies that rely on the quantities obtained here).

1. Introduction

Molecular aggregates (such as dimers, trimers, and tetramers) are often relevant to a variety of fundamental and applied fields of science.[1–10] These species bear intramolecular and/or intermolecular interactions that may act as stabilization factors for macromolecules, contributing to several of their desirable features.[11–15] For instance, Rehulka *et al.*[16] synthesized and performed *in vitro* tests on various structurally modified estradiol dimers, which are species known for possessing anticancer activity by targeting tubulin dynamics. Hai *et al.*[17] isolated a series of *ent*-kaurane diterpenoids (silvaticusins) and new silvaticusins dimers. According to the tests conducted by the authors, some of the obtained species exhibited considerable cytotoxic effects against five human tumor cell lines.[17] Xiong *et al.*[18] introduced modifications in the spike protein of SARS-CoV-2 (connected to the receptor binding and cell entry, as well as to the dominant target of the immune system), yielding the production of thermostable, disulfide-bonded S-protein trimers that can be used as reagents for serology, virology, and as immunogenic agents in serological assays.

Formaldehyde (H_2CO) is an important building block of synthetic organic chemistry, as its carbonyl group can work as an excellent hydrogen-bonding interaction acceptor.[19] On the other hand, nitroxyl (HNO) is a molecule that can be easily related (in terms of the structure) to the biomarker nitric oxide (NO), differing only by the addition of a hydrogen atom on its chemical structure and, thus, several studies have attributed an important role to HNO as an intermediate component in the biological response to NO and/or in the biosynthesis of the marker.[20–23] Both the H_2CO and HNO molecules have been detected in the interstellar medium many years ago.[24,25] Due to difficulties in the experimental isolation of the $H_2CO\cdots HNO$ dimer, with the exception of two experiments involving spectroscopy combined with entrapment in argon matrices,[26,27] the intermolecular complex between H_2CO and HNO has been studied in only a few computational investigations.[28–32] These mainly focused on probing their structural conformations, stability, and vibrational spectra. The most recent work[32] pointed to the existence of six stable conformations of the $H_2CO\cdots HNO$ dimer at the MP2/aug-cc-pVQZ level of theory.

Ionization potentials (IPs) are physical–chemical properties that may be used as auxiliary descriptors in the assignment of the different conformations of a given chemical species, as well as for probing mechanisms (at the molecular level) related to several applications.[33–35] For instance, these quantities are

[a] *Centro de Ciências da Natureza, Universidade Federal de São Carlos, Buri, São Paulo, 18290-000, Brazil. E-mail: gabriellcs@ufscar.br*
[b] *Instituto de Física, Universidade Federal de Mato Grosso, Cuiabá, Mato Grosso, 78060-900, Brazil*
[c] *Department of Chemistry, Washington State University, Pullman, Washington, 99164, USA. E-mail: kipeters@wsu.edu*

† Electronic supplementary information (ESI) available. See DOI: https://doi.org/10.1039/d4cp04442h

important for examining the single-electron-transfer (SET) and sequential proton loss electron transfer (SPLET) mechanisms that are connected to the antioxidant and other biological activities in polyphenols.[36–39] In addition, IPs can be used as input data for computing photoionization[40–42] and electron scattering[43–45] cross sections. Particularly in terms of exploring IPs and their roles in processes involving dimeric species, there has been ongoing interest of the scientific community working in physical chemistry, chemical physics, and atomic and molecular physics, in the past few years.[46–53] In terms of atomic and molecular clusters, very recently Song *et al.*[54] studied the dissociative ionization of Ar dimers with femtosecond laser fields while de Souza and Peterson investigated the ionization processes for the entire valence shells of H_2CO dimers[55] and H_2CO trimers.[56] To the best of our knowledge, no investigations on the IPs for the $H_2CO\cdots HNO$ dimer have been performed to date and, given the characteristics of this system along with the invigorated interest of the scientific community in weakly bound systems, we were motivated to perform this work.

In this work, we performed an investigation of the structures, vibrational frequencies, binding energies, and ionization potentials of the $H_2CO\cdots HNO$ dimers. A series of six different conformations were examined through the use of extensive electron correlation and sequences of correlation consistent basis sets. An illustrative representation of the chemical structures of all the conformations of the $H_2CO\cdots HNO$ dimer can be seen in Fig. 1. The relative stabilities and binding energies of the conformations were also evaluated using a more extensive level of theory compared to that used in the only other work available in the literature. It is expected that the results of the present work may motivate future experimental and computational investigations tackling the $H_2CO\cdots HNO$ dimers. In this sense, probing IPs with high accuracy, as well as vibrational frequencies, at a high level of theory may also be useful in the future identification of different conformations of dimers or determination of photoionization cross sections.

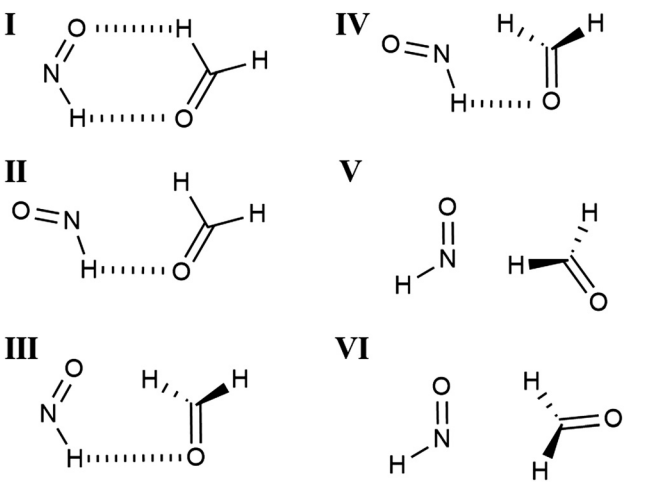

Fig. 1 Representation of the six conformations of the $H_2CO\cdots HNO$ dimers.

2. Computational methods

The geometries of six conformations of the $H_2CO\cdots HNO$ dimers as reported by Karpfen[32] at the MP2/aug-cc-pVQZ level were considered as initial guesses. The equilibrium structures of these conformers, as well as the monomers H_2CO and HNO, were then fully optimized through the use of the coupled-cluster with single, double, and perturbative triple excitations (CCSD(T)) method[57] with both the aug-cc-pVTZ and aug-cc-pVQZ[58–60] basis sets. These basis sets are denoted by aVTZ and aVQZ, respectively, below. The lowest-lying vertical IPs of all the conformations were determined for the $H_2CO\cdots HNO$ dimers using the equation-of-motion ionization potential coupled-cluster with single and double excitations method (EOMIP-CCSD)[61] with the aug-cc-pV*n*Z basis sets (n = D, T, Q) at the CCSD(T)/aVQZ geometries. Core-valence (CV) correlation effects (Δ_{CV}) were evaluated as the difference in terms of two EOMIP-CCSD computations, one considering all electrons correlated and another taking only the correlation of the valence electrons into consideration. These calculations, both the valence-only and all-electron ones, utilized the aug-cc-pCV*n*Z (n = D, T) basis sets (denoted by aCV*n*Z below) and were subsequently extrapolated to the CBS limit. The complete basis set (CBS) limits were estimated with the equation originally proposed by Martin:[62]

$$E_n = E_{CBS} + A(n + 1/2)^{-4}. \quad (1)$$

In eqn (1), the total energies were considered while n is the cardinal number related to a given basis set (*e.g.*, n = 4 in the case of the aVQZ). Finally, an adapted version[63] of the FPD composite method[64] was employed for obtaining each IP as

$$IP_{FPD} = IP_{aVTZ} + \Delta_{CBS} + \Delta_{CV}. \quad (2)$$

In eqn (2), the Δ_{CBS} contribution is obtained as the difference between a given IP determined at the EOMIP-CCSD/aVTZ basis set and its corresponding value estimated at the CBS limit, and Δ_{CV} is the CV contribution at the estimated CBS limit. The gas-phase environment was always considered in this work. The latest version of the MOLPRO[65] suite of codes was used for performing the CCSD(T) computations, while the EOMIP-CCSD results were computed with the CFOUR[66] package. The convergence criteria for all the self-consistent-field (SCF) and coupled-cluster (CC) calculations in CFOUR were set to 10^{-10} a.u. For the geometry optimizations and frequency calculations with MOLPRO, default convergence criteria were used, *i.e.*, 10^{-8} a.u. on the energies.

3. Results

In Fig. 2, the equilibrium structures of the conformations of the $H_2CO\cdots HNO$ dimer as optimized at the CCSD(T)/aVQZ level of theory are shown along with their respective bond distances and interactions. From a general perspective, all the structures obtained in the present work are in very good agreement with the corresponding MP2/aVQZ values previously reported by

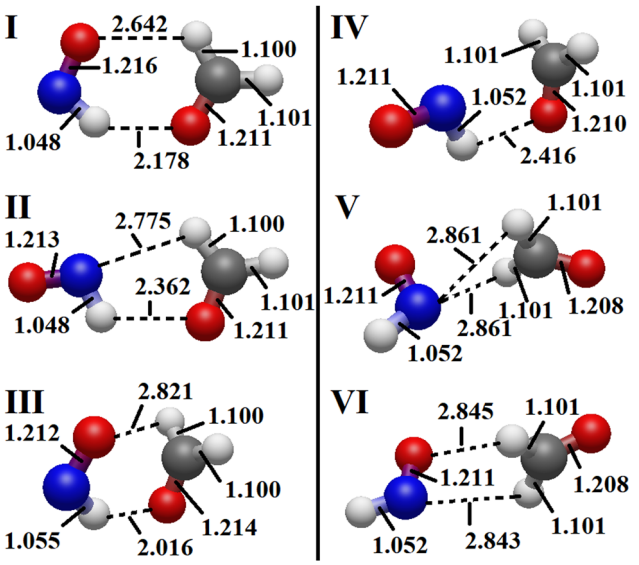

Fig. 2 Ground-state structures of six conformations of the $H_2CO\cdots HNO$ dimer optimized at the CCSD(T)/aVQZ level of theory. Inter and intramolecular bond distances are given in Å.

Karpfen.[32] The presence of hydrogen-bonding interactions (that may be formed between the hydrogen atom from HNO and the oxygen from H_2CO) is of pivotal importance for the stabilization of most of the conformations. In this sense, conformation III is suggested to present the strongest hydrogen-bonding interaction among all the $H_2CO\cdots HNO$ dimer conformations (as can be inferred from its NH$\cdots$O distance, 2.016 Å), followed by conformations I (2.178 Å), II (2.362 Å), and IV (2.416 Å); such interactions were not found in conformations V and VI.

The CCSD(T) binding energies (ΔE_b) of the different conformations of the $H_2CO\cdots HNO$ dimers, as well as their relative energies (ΔE_{conf}), are presented in Table 1. Conformer III is the strongest bound with a calculated equilibrium binding energy of -22.75 kJ mol^{-1}, which decreases in magnitude to -14.67 kJ mol^{-1} at 0 K after inclusion of zero-point energy corrections. The latter includes the small contributions from anharmonic effects taken from the MP2 study of Karpfen.[32] As shown in Table 1, conformer I lies just 0.78 kJ mol^{-1} above conformer III at 0 K while even the highest lying conformer, conformer VI, has a 0 K relative energy of 9.48 kJ mol^{-1} above conformer III. Hence all 6 conformers are likely to be populated at room temperature. Interestingly, the order of stability (III, I, II, IV, V, VI) follows an opposite trend regarding the strength of the NH$\cdots$O interactions (see Fig. 2). As also shown in Table 1, the CCSD(T)/aVTZ results for the binding energies are within 1 kJ mol^{-1} of their CBS limits in each case, suggesting the use of the aVTZ basis set as an excellence choice in terms balancing accuracy and computational cost, which can be an important factor if studies involving larger clusters of $H_2CO\cdots HNO$ are attempted in the future. In comparison to the previous results of Karpfen,[32] the present CCSD(T) results with both aVTZ and aVQZ basis sets agree very closely to his results, which is not surprising since the present CCSD(T) equilibrium geometries are not so different from the MP2 ones used in that study. Extrapolation to the CBS limit as done in this study generally leads to decreased binding energies (in magnitude) by only about 0.1–0.2 kJ mol^{-1}. The differences between the current CCSD(T) ZPE corrections and the previous MP2 results are also quite small, 0.1–0.4 kJ mol^{-1}. The study of Karpfen[32] also included CCSD(T) calculations at their MP2 geometries with both aVTZ and aVQZ basis sets (but did not include CBS extrapolations). Not surprisingly, given the closeness of the MP2 and CCSD(T) geometries, those results are nearly identical to the ones of this study.

Table 1 CCSD(T) binding energies (ΔE_b) and relative energies (ΔE_{conf}) of the 6 conformations of $H_2CO\cdots HNO$ in kJ mol^{-1}

Conformer	aVTZ	CBS	ΔZPE_{harm}	ΔZPE_{anharm}[a]	ΔE (0 K)	ΔE_{conf} (0 K)
I	−20.21	−19.52	6.23	5.63	−13.89	0.78
II	−15.73	−15.13	4.65	4.35	−10.78	3.89
III	−23.32	−22.75	9.28	8.08	−14.67	0.00
IV	−13.49	−12.97	3.81	2.91	−10.06	4.61
V	−9.54	−8.71	4.18	3.28	−5.43	9.24
VI	−9.19	−8.30	3.91	3.11	−5.19	9.48

[a] MP2 anharmonic corrections were taken from Karpfen[32] and added to the CCSD(T)/aVTZ ZPE values of this work.

In the ESI,† full sets of results are presented for the twelve lowest-lying IPs of the six conformations of $H_2CO\cdots HNO$ at the EOMIP-CCSD method with the aVDZ, aVTZ, and aVQZ basis sets. Included in these tabulations are the symmetries (in the C_s point group) of the resulting cation states. A summary of these results, as well as all FPD contributions from eqn (2), are given in Table 2. The number of IPs probed was chosen based on the work presented by Tanaka *et al.*[40] on the H_2CO molecule, which highlighted the necessity of taking into account a considerable number of inner orbitals in the calculations of its photoionization cross sections. Hence, as one of the expectations of this work is to provide important input as well as to motivate future works on photoionization by $H_2CO\cdots HNO$, it was decided to probe a considerably large number of IPs. In general, the IPs computed for all the conformations experienced a systematic increase when going from the aVDZ to the CBS limits. Taking the results of conformation III (the most stable) for example, the average difference between the aVDZ IPs and the CBS limit IPs is 0.45 eV. This average difference decreases to 0.29 eV when considering solely the six lowest-lying IPs, suggesting the use of the small double-zeta basis set as a semi-quantitative probe of the low-lying IPs. The average difference between the aVTZ and the CBS limit IPs is just 0.15 eV, which suggests the triple-zeta basis set as being an economical choice for determining the IPs of the $H_2CO\cdots HNO$ dimers. There is, however, some significant basis set dependence among the various conformers. For example, for both conformers V and VI, the average difference between the aVTZ and CBS limit IPs increases to 0.26 eV with basis set errors reaching as high as 0.36 eV in several cases for the higher IPs. A comparison of CBS limits obtained from extrapolation of aVDZ/aVTZ and aVTZ/aVQZ (the latter is shown in Table 2 and was used in the discussion of the previous paragraph) is shown in the ESI.† Overall good agreement can be observed between the CBS[DT] and CBS[TQ] results, *i.e.*, for

Table 2 Vertical IPs of the $H_2CO\cdots HNO$ dimers as determined using the FPD approach. The values are given in eV

Conformation	I	II	III	IV	V	VI
IP 1						
E_{aVTZ}	9.88	10.01	10.31	10.25	10.43	10.44
$\Delta_{CBS[TQ]}$	0.13	0.17	0.11	0.19	0.23	0.23
Δ_{CV}	0.03	0.04	0.04	0.04	0.03	0.03
IP_{FPD}	10.05	10.22	10.46	10.48	10.69	10.69
IP 2						
E_{aVTZ}	11.25	11.20	10.93	10.98	10.86	10.88
$\Delta_{CBS[TQ]}$	0.12	0.16	0.11	0.19	0.23	0.24
Δ_{CV}	0.03	0.03	0.03	0.03	0.04	0.04
IP_{FPD}	11.40	11.39	11.08	11.20	11.13	11.16
IP 3						
E_{aVTZ}	14.85	14.83	14.32	14.59	14.18	14.20
$\Delta_{CBS[TQ]}$	0.10	0.14	0.10	0.17	0.20	0.21
Δ_{CV}	0.03	0.03	0.04	0.03	0.03	0.03
IP_{FPD}	14.98	15.01	14.46	14.79	14.42	14.44
IP 4						
E_{aVTZ}	15.52	15.65	16.02	15.95	15.65	15.64
$\Delta_{CBS[TQ]}$	0.13	0.17	0.12	0.19	0.23	0.23
Δ_{CV}	0.04	0.04	0.04	0.04	0.03	0.03
IP_{FPD}	15.69	15.86	16.17	16.18	15.91	15.91
IP 5						
E_{aVTZ}	16.20	16.36	16.19	16.27	16.49	16.51
$\Delta_{CBS[TQ]}$	0.09	0.13	0.11	0.19	0.24	0.24
Δ_{CV}	0.03	0.03	0.04	0.03	0.04	0.04
IP_{FPD}	16.33	16.53	16.34	16.49	16.76	16.79
IP 6						
E_{aVTZ}	16.41	16.38	16.53	16.54	16.96	16.96
$\Delta_{CBS[TQ]}$	0.12	0.16	0.08	0.16	0.20	0.21
Δ_{CV}	0.03	0.03	0.03	0.03	0.03	0.03
IP_{FPD}	16.57	16.58	16.64	16.73	17.19	17.19
IP 7						
E_{aVTZ}	16.79	16.88	17.27	17.11	17.19	17.21
$\Delta_{CBS[TQ]}$	0.25	0.29	0.23	0.31	0.20	0.21
Δ_{CV}	0.16	0.16	0.16	0.16	0.03	0.03
IP_{FPD}	17.20[a]	17.34[a]	17.66[a]	17.59[a]	17.43	17.45
IP 8						
E_{aVTZ}	17.51	17.65	17.54	17.59	17.75	17.77
$\Delta_{CBS[TQ]}$	0.10	0.14	0.09	0.16	0.35	0.36
Δ_{CV}	0.03	0.03	0.03	0.03	0.17	0.17
IP_{FPD}	17.64	17.82	17.66	17.78	18.27[a]	18.30[a]
IP 9						
E_{aVTZ}	18.29	18.24	18.57	18.36	18.16	18.16
$\Delta_{CBS[TQ]}$	0.11	0.16	0.11	0.18	0.35	0.35
Δ_{CV}	0.03	0.03	0.02	0.02	0.14	0.14
IP_{FPD}	18.43	18.42	18.70	18.56	18.65[a]	18.65[a]
IP 10						
E_{aVTZ}	18.92	18.70	18.80	18.54	18.93	18.95
$\Delta_{CBS[TQ]}$	0.24	0.29	0.23	0.32	0.23	0.23
Δ_{CV}	0.14	0.14	0.16	0.16	0.04	0.04
IP_{FPD}	19.30[a]	19.13[a]	19.19[a]	19.01[a]	19.19[a]	19.21[a]
IP 11						
E_{aVTZ}	20.32	20.00	20.30	19.88	19.56	19.57
$\Delta_{CBS[TQ]}$	0.25	0.29	0.23	0.32	0.35	0.36
Δ_{CV}	0.14	0.14	0.14	0.14	0.14	0.14
IP_{FPD}	20.70[a]	20.44[a]	20.67[a]	20.34[a]	20.05[a]	20.06[a]
IP 12						
E_{aVTZ}	20.67	20.70	20.92	20.61	20.89	20.89
$\Delta_{CBS[TQ]}$	0.24	0.28	0.23	0.30	0.35	0.32
Δ_{CV}	0.13	0.13	0.13	0.13	0.14	0.12
IP_{FPD}	21.05[a]	21.12[a]	21.29[a]	21.05[a]	21.38[a]	21.33[a]

[a] Two-electron transition.

conformation III, the average difference between was calculated to be just 0.048 eV. This observation is important for future investigations tackling larger $H_2CO\cdots HNO$ clusters where computational cost may be an issue.

One effect that has been mostly neglected in this work is the contribution of scalar relativity to the calculated IPs. While this is expected to be small for these light elements, a limited number of calculations were carried out on the 1st IPs of each conformation. In these calculations the contribution due to scalar relativity was calculated as the difference in IPs at the CCSD level of theory using the aVTZ basis sets for the non-relativistic case and the aug-cc-pVTZ-DK basis sets[67] with the 2nd-order Douglas–Kroll–Hess scalar relativistic Hamiltonian[68,69] in the other. These calculations confirmed that the effect is very small for the IPs of these molecules, whereby the inclusion of scalar relativity decreased the non-relativistic IPs by about 0.005 eV in every case.

In Table 2, the final FPD IPs are presented for each conformation of the $H_2CO\cdots HNO$ dimer along with their respective contributions in terms of CBS limit extrapolated values and core correlation effects. Core correlation is observed to increase all the lower IPs by only about 0.03 to 0.04 eV, but basis sets of at least aCVTZ are required. For the higher IPs, the effects of correlating the core electrons increase to as much as 0.17 eV. Comparing the CBS limits of Δ_{CV} to these contributions calculated with the aCVTZ basis set, the latter tends to underestimate the core correlation contributions by 0.01 to 0.04 eV. The first FPD IP computed for conformation III (the most stable) was determined to be 10.46 eV. The first IPs of conformations I, II, and IV were calculated to differ from the value obtained for conformation III by −0.41 eV, −0.24 eV, and +0.02 eV, respectively. These differences may be helpful to the assignments of experimental results. On the other hand, the first IPs of conformations V and VI were determined as being identical (10.69 eV), which can suggest an eventual identification/differentiation between these conformations based on their IPs as not being possible; this behavior was also observed for the other eleven low-lying IPs of conformations V and VI, which presented identical (or nearly identical) values. The conformation I exhibited the lowest IPs seven times among all the conformations. In terms of general trends for a given IP of the conformations, the order I, II, III, IV, V = VI was noticed three times (with the IP of conformation I being the lowest). Unfortunately, no experimental results of IPs are available in the literature (to our knowledge) for the $H_2CO\cdots HNO$ dimer. However, the FPD method is well-known for being able to provide results of thermochemical and spectroscopic properties in excellent agreement (*i.e.*, within the chemical accuracy, $\approx$0.043 eV) when compared to experimental data[70,71] and,

thus, the outcomes from this work may serve as motivation for IP measurements to be attempted in the future.

In an effort to better understand the cationic dimers of this work, adiabatic IPs for all the conformations of the $H_2CO\cdots HNO^+$ dimer cations were determined by geometry optimizations (in C_1 symmetry) and subsequent harmonic frequency calculations at the R/UCCSD(T)/aVTZ level of theory (restricted open-shell Hartree–Fock orbitals with unrestricted CCSD as implemented in Molpro[72]). The resulting CCSD adiabatic IPs for dimers I–VI are (in eV) 7.83, 7.79, 7.84, 7.76, 9.56, and 10.10, respectively. Compared to the 1st vertical IPs of Table 2 calculated with EOMIP-CCSD, the adiabatic IPs of dimers I–IV are smaller by over 2 eV, reflecting the large geometry changes upon ionization. The geometry changes for dimers V and particularly VI are more modest, as reflected in adiabatic IPs smaller than their vertical ones by 0.9 and 0.3 eV, respectively. As shown in Fig. 3, the cations of dimers I–IV all have the same final equilibrium geometries, whereby a proton is transferred from the HNO fragment to H_2CO, leaving an NO radical complexing with H_2COH^+. This results in a strong interaction between the proton and the N atom of the NO fragment, as indicated by a H···N distance of just 1.728 Å. In contrast, the formation of H_2 $C(O)N(O)H^+$ is observed when the electron is ejected from conformation V of the $H_2CO\cdots HNO$ dimer (unpaired electron on the O of H_2CO), while conformation VI presented a cationic structure bearing a hydrogen-bonding interaction between the O atom from HNO and the H atom from H_2CO that is stronger than the corresponding interaction noticed previously for its neutral form due to the positive charge on the HNO fragment (the unpaired electron is localized on the O atom of HNO).

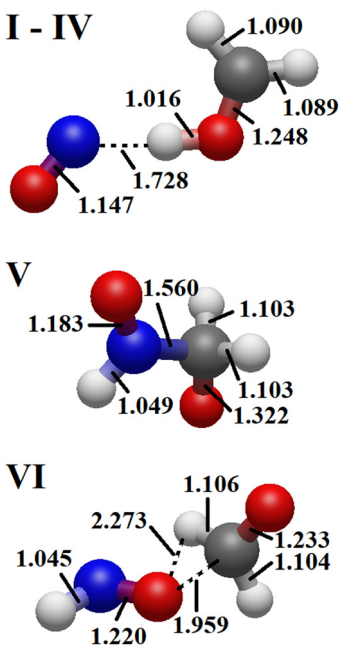

Fig. 3 Structures of the cationic forms of the $H_2CO\cdots HNO$ dimer as optimized at the CCSD(T)/aVTZ level of theory. Inter- and intramolecular bond distances are given in Å.

Table 3 Vertical IPs of the H_2CO and HNO monomers as determined using the FPD approach (eV)

Species	State symmetry	E_{aVTZ}	$\Delta_{CBS[TQ]}$	Δ_{CV}	IP_{FPD}
H_2CO[a]					
	A′	10.85	0.12	0.02	10.99[b]
	A″	14.58	0.09	0.03	14.70[b]
	A′	16.09	0.12	0.03	16.24[b]
	A′	17.46	0.10	0.02	17.58[b]
	A″	21.21	0.21	0.18	21.59[c]
	A′	21.80	0.08	0.07	21.95[c]
HNO					
	A′	10.46	0.12	0.04	10.62
	A′	16.03	0.13	0.04	16.20
	A″	16.74	0.09	0.04	16.87
	A″	17.22	0.25	0.16	17.62[c]
	A′	18.54	0.12	0.03	18.70
	A′	21.74	0.22	0.15	22.11[c]
	A″	22.31	0.26	0.16	22.73[c]

[a] Symmetries are given in the C_s point group to assist the interpretation of the dimer. [b] Results taken from ref. 55. [c] Two-electron transition.

Last, Table 3 shows the calculated EOMIP-CCSD IPs for the monomers H_2CO and HNO using the same methodology as the dimers. In addition, Fig. S1 in the ESI† shows the molecular orbitals of the all 6 dimer conformations, as well as the monomers, from the highest occupied molecular orbital (HOMO) to the HOMO−6. From this figure it is clear that in many cases the ionization is localized to only one monomer, but in some cases the molecular orbital from which ionization occurs is spread over the whole dimer.

4. Conclusions

A computational investigation on the structures and ionization potentials of the $H_2CO\cdots HNO$ dimer was presented. The equilibrium structures of six conformations of the clusters were examined using the CCSD(T)/aVTZ and CCSD(T)/aVQZ approaches. The conformation III showed the strongest hydrogen-bonding interaction among the dimers and was determined as being the most stable, although all the other conformations were found to be considerably close in terms of relative energies. Twelve lowest-lying IPs were evaluated for each conformation through the use of the EOMIP-CCSD method along with correlation consistent basis sets, extrapolation to the CBS limit and taking core correlation effects into account. The differences noticed in the IPs of the conformations may be helpful to the assignments of experimental results regarding identification of the $H_2CO\cdots HNO$ dimers. The outcomes from this work will hopefully serve as motivation for other experimental and theoretical investigations involving $H_2CO\cdots HNO$ dimers (that rely on the quantities obtained here) to be performed.

Data availability

The code for computing the vertical ionization potentials can be found at **https://cfour.uni-mainz.de/cfour/** – D. A. Matthews, L. Cheng, M. E. Harding, F. Lipparini, S. Stopkowicz, T.-C.

Jagau, P. G. Szalay, J. Gauss, J. F. Stanton, 2020, *J. Chem. Phys.* **152:** 214108, DOI: **https://doi.org/10.1063/5.0004837**. The version of the code employed for this study is version 2.1. The code used for electronic structure computations can be found at **https://www.molpro.net** – H.-J. Werner, P. J. Knowles, F. R. Manby, J. A. Black, K. Doll, A. Heßelmann, D. Kats, A. Köhn, T. Korona, D. A. Kreplin, Q. Ma, T. F Miller 3rd, A. Mitrushchenkov, K. A. Peterson, I. Polyak, G. Rauhut, M. Sibaev, 2020, *J. Chem. Phys.* **152:** 144107, DOI: **https://doi.org/10.1063/5.0005081**. The version of the code employed for this study is version 2024.2.

Conflicts of interest

There are no conflicts to declare.

Acknowledgements

Professor Gabriel L. C. de Souza thanks the Brazilian funding agencies Fundação de Amparo à Pesquisa do Estado de São Paulo, FAPESP, (grant 2023/11043-4) and Conselho Nacional de Desenvolvimento Científico e Tecnológico, CNPq, (grants 305401/2022-0 and 403961/2021-1) for providing the financial resources required for developing this work.

References

1 P. Soulard and B. Tremblay, *J. Mol. Struct.*, 2025, **1321**, 140040.
2 S. Y. Peng, Y. D. Yang, R. Tian and N. H. Lu, *J. Environ. Sci.*, 2025, **149**, 88.
3 B. P. Zhu, H. W. Ge, J. H. Wei, Y. Xu, S. L. Wang, B. Li and H. F. Xu, *Ind. Crops Prod.*, 2024, **222**, 119736.
4 H. C. Zhang, Z. N. Liu and H. Fu, *Nanomaterials*, 2020, **10**, 651.
5 R. Z. Yao, S. Lan and G. C. Li, *J. Phys. D: Appl. Phys.*, 2025, **58**, 015101.
6 M. Ghuneim and R. W. Bomantara, *J. Condens. Matter Phys.*, 2024, **36**, 495402.
7 X. N. Feng, J. S. Zhang, J. S. Liu, J. Y. Su, X. R. Liu, M. W. Yang, Y. L. Peng, H. Z. Yan and Z. L. Chen, *Clin. Chim. Acta*, 2025, **565**, 119967.
8 Z. F. Liu, X. X. Liu, H. Zhang, L. Zeng, L. Y. Niu, P. Z. Chen, W. H. Fang, X. J. Peng, G. L. Cui and Q. Z. Yang, *Angew. Chem., Int. Ed.*, 2024, **63**, e202407135.
9 M. L. Liu, B. J. Wang, S. J. Yi, X. X. Dou, Y. Q. Zhang, H. Yu, X. L. Zhang, S. Y. Dong, J. L. Feng, Z. G. Cao and L. Y. Zhu, *Environ. Int.*, 2024, **192**, 109053.
10 P. E. Prasad, N. Dhore, A. Palanisamy and C. P. K. Rao, *Prog. Org. Coat.*, 2024, **197**, 108802.
11 B. Qiao, L. Lopez and M. O. de la Cruz, *J. Phys. Chem. B*, 2019, **123**, 3907.
12 C. Scaletti, P. P. S. Russel, K. J. Hebel, M. M. Rickard, M. Boob, F. Danksagmüller, S. A. Taylor, T. V. Pogorelov and M. Gruebele, *Proc. Natl. Acad. Sci. U. S. A.*, 2024, **121**, e2319094121.
13 J. L. F. Santos, A. C. Kauffmann, S. C. da Silva, V. C. P. Silva and G. L. C. de Souza, *J. Mol. Model.*, 2020, **26**, 233.
14 D. Mallamace, E. Fazio, F. Mallamace and C. Corsaro, *Int. J. Mol. Sci.*, 2018, **19**, 3825.
15 A. H. da, S. Filho, F. S. Candeias, S. C. da Silva, F. C. Vicentini, M. H. T. Assumpção, A. Brown and G. L. C. de Souza, *J. Mol. Model.*, 2020, **26**, 309.
16 J. Rehulka, M. Jurásek, P. Dráber, A. Ivanová, S. Gurská, K. Jecmenová, O. Mokshyna, M. Hajdúch, P. Polishchuk, P. B. Drasar and P. Dzubák, *J. Enzyme Inhib. Med. Chem.*, 2024, **39**, 2367139.
17 Q. X. Hai, K. Hu, S. P. Chen, Y. Y. Fu, X. N. Li, H. D. Sun, H. P. He and P. T. Puno, *Nat. Prod. Bioprospect.*, 2024, **14**, 45.
18 X. Xiong, K. Qu, K. A. Ciazynska, M. Hosmillo, A. P. Carter, S. Ebrahimi, Z. Ke, S. H. W. Scheres, L. Bergmaschi, G. L. Grice, Y. Zhang, The CITIID-NIHR COVID-19 BioResource Collaboration, J. A. Nathan, S. Baker, L. C. James, H. E. Baxendale, I. Goodfellow, R. Doffinger and J. A. G. Briggs, *Nat. Struct. Mol. Biol.*, 2020, **27**, 934.
19 S. Scheiner, *Hydrogen Bonding*, Oxford Univ. Press, 1997, 89–103.
20 B. K. Kemp-Harper, A. Velagic, N. Paolocci, J. D. Horowitz and R. H. Ritchie, *Handb. Exp. Pharmacol.*, 2021, **264**, 311.
21 R. Michalski, R. Smulik-Izydorczyk, J. Pieta, M. Rola, A. Artelska, K. Pierzchala, J. Zielonka, B. Kalyanarama and A. B. Sikora, *Front. Chem.*, 2022, **5**, 930657.
22 J. M. Fukuto, C. J. Cisneros and R. L. Kinkade, *J. Inorg. Biochem.*, 2013, **118**, 201.
23 S. K. Stöckl, R. de Col, M. R. Filipovic and K. Messlinger, *Int. J. Mol. Sci.*, 2022, **23**, 230.
24 L. E. Snyder, D. Buhl, B. Zuckerman and P. Palmer, *Phys. Rev. Lett.*, 1969, **22**, 679.
25 B. L. Ulich, J. M. Hollis and L. E. Snyder, *Astrophys. J.*, 1977, **217**, L105.
26 R. P. Müller, P. Russegger and J. R. Huber, *Chem. Phys.*, 1982, **70**, 281.
27 M. E. Jacox, *J. Phys. Chem.*, 1984, **88**, 3373.
28 Y. Liu, W. Q. Liu, H. Y. Li, Y. Yang and S. Cheng, *Chin. J. Chem.*, 2007, **25**, 44.
29 T. T. Nguyen, T. T. Hue and M. T. Nguyen, *J. Phys. Chem. A*, 2009, **113**, 3245.
30 Y. Yang and Y. Liu, *Int. J. Quantum Chem.*, 2010, **110**, 1264.
31 X. L. Kong, *Acta Phys. Chim. Sin.*, 2012, **28**, 303.
32 A. Karpfen, *Comput. Theor. Chem.*, 2017, **1108**, 10.
33 S. Dutta, N. R. Behera, S. Barik, R. K. Kushawaha, Y. Sajeev and G. Aravind, *J. Chem. Phys.*, 2024, **161**, 124302.
34 J. L. Fischer, K. N. Blodgett, C. P. Harrilal, P. S. Walsh, Z. S. Davis, S. Choi, S. H. Choi and T. S. Zwier, *J. Phys. Chem. A*, 2022, **126**, 1837.
35 Y. R. Lee, H. L. Kim and C. H. Kwon, *Phys. Chem. Chem. Phys.*, 2020, **22**, 6184.
36 G. L. C. de Souza and K. A. Peterson, *J. Phys. Chem. A*, 2021, **125**, 198.
37 R. A. Mendes, S. K. C. Almeida, I. N. Soares, C. A. Barboza, R. G. Freitas, A. Brown and G. L. C. de Souza, *J. Mol. Model.*, 2019, **25**, 89.

38 I. N. Soares, K. A. Peterson and G. L. C. de Souza, *J. Phys. Chem. A*, 2024, **128**, 2727.
39 R. A. Mendes, V. A. S. da Mata, A. Brown and G. L. C. de Souza, *Phys. Chem. Chem. Phys.*, 2024, **26**, 8613.
40 H. K. Tanaka, F. V. Prudente, A. Medina, R. R. T. Marinho, M. G. P. Homem, L. E. Machado and M. M. Fujimoto, *J. Chem. Phys.*, 2017, **146**, 094310.
41 J. S. Murray and N. T. Clemens, *J. Chem. Phys.*, 2024, **160**, 244302.
42 J. Huang, C. Huang, X. Wu, Q. Hou, G. Tian, J. Yang and F. Zhang, *J. Chem. Phys.*, 2021, **154**, 244301.
43 R. T. Sugohara, M. G. P. Homem, I. Iga, G. L. C. de Souza, L. E. Machado, J. R. Ferraz, A. S. dos Santos, L. M. Brescansin, R. R. Lucchese and M.-T. Lee, *Phys. Rev. A*, 2013, **88**, 022709.
44 E. A. Y. Castro, G. L. C. de Souza, I. Iga, L. E. Machado, L. M. Brescansin and M.-T. Lee, *J. Electron Spectrosc. Relat. Phenom.*, 2007, **159**, 30.
45 M.-T. Lee, I. Iga, L. E. Machado, L. M. Brescansin, E. A. Y. Castro and G. L. C. de Souza, *Phys. Rev. A*, 2006, **74**, 052716.
46 M. Busch and M. Sotoudeh, *J. Chem. Phys.*, 2023, **159**, 034303.
47 M. Stadlhofer, B. Thaler and M. Koch, *Phys. Chem. Chem. Phys.*, 2022, **24**, 24727.
48 I. S. Vinklárek, H. Bromberger, N. Vadassery, W. Jin, J. Küpper and S. Trippel, *J. Phys. Chem. A*, 2024, **128**, 1593.
49 C. Joblin, L. Dontot, G. A. Garcia, F. Spiegelman, M. Rapacioli, L. Nahon, P. Parneix, T. Pino and P. Bréchignac, *J. Phys. Chem. Lett.*, 2017, **8**, 3697.
50 M. H. Shi, C. X. Lu, S. Z. Pan, L. R. Zhou, H. C. Ni, P. F. Lu, W. B. Zhang and J. Wu, *Phys. Rev. A*, 2023, **108**, 043108.
51 X. G. Ren, K. Hossen, S. K. Jia, J. Q. Zhou, X. R. Xue, T. Pfeifer and A. Dorn, *Phys. Rev. A*, 2024, **110**, 042801.
52 X. T. Yu, X. Y. Zhang, X. Q. Hu, X. N. Zhao, D. X. Ren, X. K. Li, P. Ma, C. C. Wang, Y. Wu, S. Z. Luo and D. J. Ding, *Phys. Rev. Lett.*, 2022, **129**, 023001.
53 E. R. Molina, B. Xu, O. Kostko, M. Ahmed and T. Stein, *Phys. Chem. Chem. Phys.*, 2022, **24**, 23106.
54 P. Song, Y. L. Zhu, X. W. Wang, C. S. Meng, T. Jiang, Z. H. Lv, D. W. Zhang, C. C. Qin, Z. X. Zhao and J. M. Yuan, *Sci. China: Phys., Mech. Astron.*, 2024, **67**, 123011.
55 G. L. C. de Souza and K. A. Peterson, *J. Chem. Phys.*, 2020, **152**, 194305.
56 G. L. C. de Souza and K. A. Peterson, *J. Chem. Phys.*, 2021, **155**, 084304.
57 K. Raghavachari, G. W. Trucks, J. A. Pople and M. Head-Gordon, *Chem. Phys. Lett.*, 1989, **157**, 479.
58 T. H. Dunning, *J. Chem. Phys.*, 1989, **90**, 1007.
59 R. A. Kendall, T. H. Dunning and R. J. Harrison, *J. Chem. Phys.*, 1992, **96**, 6796.
60 D. E. Woon and T. H. Dunning, *J. Chem. Phys.*, 1995, **103**, 4572.
61 J. F. Stanton and R. J. Bartlett, *J. Chem. Phys.*, 1993, **98**, 7029.
62 J. M. L. Martin, *Chem. Phys. Lett.*, 1996, **259**, 669.
63 G. L. C. de Souza and K. A. Peterson, *Phys. Chem. Chem. Phys.*, 2022, **24**, 17751.
64 D. A. Dixon, D. Feller and K. A. Peterson, *Annu. Rep. Comput. Chem.*, 2012, **8**, 1.
65 H.-J. Werner, P. J. Knowles, F. R. Manby, J. A. Black, K. Doll, A. HeÃŸelmann, D. Kats, A. Köhn, T. Korona, D. A. Kreplin, Q. Ma, T. F. MillerIII, A. Mitrushchenkov, K. A. Peterson, I. Polyak, G. Rauhut and M. Sibaev, *J. Chem. Phys.*, 2020, **152**, 144107.
66 J. F. Stanton, J. Gauss, L. Cheng, M. E. Harding, D. A. Matthews, P. G. Szalay with contributions from A. A. Auer, R. J. Bartlett, U. Benedikt, C. Berger, D. E. Bernholdt, Y. J. Bomble, O. Christiansen, F. Engel, R. Faber, M. Heckert, O. Heun, M. Hilgenberg, C. Huber, T.-C. Jagau, D. Jonsson, J. Jusélius, T. Kirsch, K. Klein, W. J. Lauderdale, F. Lipparini, T. Metzroth, L. A. Mück, D.P. O'Neill, D. R. Price, E. Prochnow, C. Puzzarini, K. Ruud, F. Schiffmann, W. Schwalbach, C. Simmons, S. Stopkowicz, A. Tajti, J. Vázquez, F. Wang, J. D. Watts and the integral packages MOLECULE (J. Almlö and P. R. Taylor), PROPS (P.R. Taylor), ABACUS (T. Helgaker, H. J. Aa. Jensen, P. Jörgensen, and J. Olsen), and ECP routines by A. V. Mitin and C. van Wüllen. For the current version, see **https://www.cfour.de**.
67 W. A. de Jong, R. J. Harrison and D. A. Dixon, *J. Chem. Phys.*, 2011, **114**, 48.
68 M. Douglas and N. M. Kroll, *Ann. Phys.*, 1974, **82**, 89.
69 G. Jansen and B. A. Hess, *Phys. Rev. A*, 1989, **39**, 6016.
70 D. Feller and E. R. Davidson, *J. Chem. Phys.*, 2018, **148**, 234308.
71 M. Vasiliu, K. A. Peterson, K. O. Christe and D. A. Dixon, *Inorg. Chem.*, 2019, **58**, 8279.
72 P. J. Knowles, C. Hampel and H. J. Werner, *J. Chem. Phys.*, 1993, **99**, 5219.

